Multipole Transforms

David Kirkby

Affiliation not available

December 16, 2019

1 Introduction

Our goal is efficient and robust numerical evaluation of Fourier integrals of the form

$$f(\vec{r}) = N_n(a,b) \int d^n k \, e^{+bi(\vec{k}\cdot\vec{r})} \, \tilde{f}(\vec{k}) \quad , \quad \tilde{f}(\vec{k}) = \tilde{N}_n(a,b) \int d^n r \, e^{-bi(\vec{k}\cdot\vec{r})} \, f(\vec{r}) \; , \tag{1}$$

with normalization factors

$$N_n(a,b) = |b|^{n/2} (2\pi)^{-n(1+a)/2} \quad , \quad \tilde{N}_n(a,b) = |b|^{n/2} (2\pi)^{-n(1-a)/2} \; , \tag{2}$$

where the constants a and b establish our choice of Fourier convention[1]. We focus on two- and three-dimensional ($n = 2, 3$) transforms of functions that can be adequately represented with a small number of (not necessarily low order) multipoles. Specifically, for $n = 2$, we expand

$$f(r,\varphi_r) = \sum_{m=-\infty}^{+\infty} f_m(r) \, \Phi_m(\varphi_r) \quad , \quad \tilde{f}(k,\varphi_k) = \sum_{m=-\infty}^{+\infty} \tilde{f_m}(k) \, \Phi_m(\varphi_k) \; , \tag{3}$$

using the polar basis functions

$$\Phi_m(\varphi) \equiv \frac{1}{\sqrt{2\pi}} \, e^{im\varphi} \tag{4}$$

with orthonormality[2] (δ_D and δ are the Dirac and Kronecker delta functions, respectively):

$$\sum_{m=-\infty}^{+\infty} \Phi_m(\varphi) \Phi_m^*(\varphi') = \delta_D(\varphi - \varphi') \tag{5}$$

[1] Use $a = 1$ and $b = 1$ for the convention of references [1, 4].

[2] `http://dlmf.nist.gov/1.17E12`

and

$$\int_0^{2\pi} d\varphi\, \Phi_m(\varphi)\Phi^*_{m'}(\varphi) = \delta_{mm'} \ . \tag{6}$$

Similarly, for $n = 3$, we expand

$$f(r,\theta_r,\varphi_r) = \sum_{\ell=0}^{\infty}\sum_{m=-\ell}^{+\ell} f_{\ell m}(r)\, Y_{\ell m}(\theta_r,\varphi_r) \quad , \quad \tilde{f}(k,\theta_k,\varphi_k) = \sum_{\ell=0}^{\infty}\sum_{m=-\ell}^{+\ell} \tilde{f_{\ell m}}(k)\, Y_{\ell m}(\theta_k,\varphi_k) \ , \tag{7}$$

using the spherical-harmonic basis functions[3] (with associated Legendre polynomials P_ℓ^m)

$$Y_{\ell m}(\theta,\varphi) \equiv \sqrt{\frac{2\ell+1}{2}\frac{(\ell-m)!}{(\ell+m)!}}\, P_\ell^m(\cos\theta)\Phi_m(\varphi) \tag{8}$$

with orthonormality[4]

$$\sum_{\ell=0}^{\infty}\sum_{m=-\ell}^{+\ell} Y_{\ell m}(\theta,\varphi)Y^*_{\ell m}(\theta',\varphi') = \delta_D(\cos\theta-\cos\theta')\delta_D(\varphi-\varphi') \tag{9}$$

and[5]

$$\int d\Omega\, Y_{\ell m}(\theta,\varphi)Y^*_{\ell' m'}(\theta,\varphi) = \delta_{\ell\ell'}\delta_{mm'} \ . \tag{10}$$

In the special case of a three-dimensional $f(\vec{r})$ that is cylindrically symmetric, *i.e.* has no ϕ_r dependence, only $m = 0$ terms contribute to the multipole expansion equation 7. Since

$$Y_{\ell 0}(\theta,\varphi) = \sqrt{\frac{2\ell+1}{4\pi}}\, L_\ell(\mu) \tag{11}$$

with L_ℓ the Legendre polynomial and $\mu \equiv \cos\theta$, it is then convenient to replace equation 7 with the equivalent expansion

$$f(r,\mu_r) = \sum_{\ell=0}^{\infty} f_\ell^{(\mu)}(r)L_\ell(\mu_r) \quad , \quad \tilde{f}(k,\mu_k) = \sum_{\ell=0}^{\infty} \tilde{f}_\ell^{(\mu)}(k)L_\ell(\mu_k) \ , \tag{12}$$

in which the coefficient functions are simply rescaled

$$f_\ell^{(\mu)}(r) = \sqrt{\frac{2\ell+1}{4\pi}}\, f_{\ell 0}(r) \quad , \quad \tilde{f}_\ell^{(\mu)}(k) = \sqrt{\frac{2\ell+1}{4\pi}}\, \tilde{f_{\ell 0}}(k) \ . \tag{13}$$

Our general approach is to translate the multi-dimensional Fourier transform, equation 1, into a small number (one per multipole) of one-dimensional

[3] `http://dlmf.nist.gov/14.30E1`
[4] `http://dlmf.nist.gov/1.17E25`
[5] `http://dlmf.nist.gov/14.30E8`

Hankel ($n = 2$) or spherical Bessel ($n = 3$) transforms between the weight functions $f_m(r)$ and $\tilde{f_m}(k)$ or $f_{\ell m}(r)$ and $\tilde{f_{\ell m}}(k)$. We derive these transforms below then, in the following sections, describe our numerical algorithm for calculating them. Note that we rely on the fact that the Fourier transform does not mix the multipoles, so that there is a one-to-one correspondence between modes in r-space and k-space.

Using equation 6, we find for $n = 2$

$$f_m(r) = \int_0^{2\pi} d\varphi_r \, f(r, \varphi_r) \, \Phi_m^*(\varphi_r) \quad , \quad \tilde{f_m}(k) = \int_0^{2\pi} d\varphi_k \, \tilde{f}(k, \varphi_k) \, \Phi_m^*(\varphi_k) \tag{14}$$

and similarly for $n = 3$ using equation 10

$$f_{\ell m}(r) = \int d\Omega_r \, f(r, \theta_r, \varphi_r) \, Y_{\ell m}^*(\theta_r, \varphi_r) \quad , \quad \tilde{f_{\ell m}}(k) = \int d\Omega_k \, \tilde{f}(k, \theta_k, \varphi_k) \, Y_{\ell m}^*(\theta_k, \varphi_k) \; . \tag{15}$$

In the case of $n = 3$ cylindrical symmetric, equations 11 and 13 yield the equivalent

$$f_\ell^{(\mu)}(r) = \frac{2\ell + 1}{2} \int_{-1}^{+1} d\mu_r \, f(r, \mu_r) \, L_\ell(\mu_r) \quad , \quad \tilde{f}_\ell^{(\mu)}(k) = \frac{2\ell + 1}{2} \int_{-1}^{+1} d\mu_k \, \tilde{f}(k, \mu_k) \, L_\ell(\mu_k) \; . \tag{16}$$

Next, we replace $f(r, \varphi_r)$ or $f(r, \theta_r, \varphi_r)$ in these equations with their Fourier expansions of equation 1, obtaining

$$f_m(r) = N_n(a, b) \int_0^\infty k dk \int_0^{2\pi} d\varphi_r \int_0^{2\pi} d\varphi_k \, e^{+bi(\vec{k} \cdot \vec{r})} \, \tilde{f}(k, \varphi_k) \, \Phi_m^*(\varphi_r) \tag{17}$$

and

$$f_{\ell m}(r) = N_n(a, b) \int_0^\infty k^2 dk \int d\Omega_r \int d\Omega_k \, e^{+bi(\vec{k} \cdot \vec{r})} \, \tilde{f}(k, \theta_k, \varphi_k) \, Y_{\ell m}^*(\theta_r, \varphi_r) \; . \tag{18}$$

Substituting the multipole expansions of $\tilde{f}$ from equations 3 and 7, we find

$$f_m(r) = N_n(a, b) \int_0^\infty k dk \int_0^{2\pi} d\varphi_r \int_0^{2\pi} d\varphi_k \, e^{+bi(\vec{k} \cdot \vec{r})} \sum_{m'=-\infty}^{+\infty} \tilde{f_{m'}}(k) \, \Phi_{m'}(\varphi_k) \, \Phi_m^*(\varphi_r) \tag{19}$$

and

$$f_{\ell m}(r) = N_n(a, b) \int_0^\infty k^2 dk \int d\Omega_r \int d\Omega_k \, e^{+bi(\vec{k} \cdot \vec{r})} \sum_{\ell'=0}^{\infty} \sum_{m'=-\ell'}^{+\ell'} \tilde{f_{\ell' m'}}(k) \, Y_{\ell' m'}(\theta_k, \varphi_k) \, Y_{\ell m}^*(\theta_r, \varphi_r) \; . \tag{20}$$

Finally we expand the plane wave factor in terms of polar ($n = 2$) basis functions

$$e^{+bi(\vec{k} \cdot \vec{r})} = 2\pi \sum_{m=-\infty}^{+\infty} (bi)^m \, J_m(kr) \, \Phi_m^*(\varphi_r) \, \Phi_m(\phi_k) \tag{21}$$

or spherical harmonic ($n = 3$) basis functions

$$e^{+bi(\vec{k}\cdot\vec{r})} = 4\pi \sum_{\ell=0}^{\infty} \sum_{m=-\ell}^{+\ell} (bi)^{\ell} j_{\ell}(kr)\, Y^{*}_{\ell m}(\theta_r, \varphi_r)\, Y_{\ell m}(\theta_k, \varphi_k) \;, \tag{22}$$

where J_m and j_ℓ are the Bessel and spherical Bessel functions, respectively. Using equations 5 or 9 to simplify the resulting expressions, we find that the moments of f and $\tilde{f}$ are related by a scaled Hankel transform when $n = 2$,

$$f_m(r) = c \int_0^{\infty} k dk\, J_m(kr)\, \tilde{f_m}(k) \quad , \quad c = 2\pi N_n(a,b)(bi)^m \;, \tag{23}$$

and by a scaled spherical Bessel transform when $n = 3$,

$$f_{\ell m}(r) = c \int_0^{\infty} k^2 dk\, j_{\ell}(kr)\, \tilde{f_{\ell m}}(k) \quad , \quad c = 4\pi N_n(a,b)(bi)^{\ell} \;. \tag{24}$$

Substituting $f \leftrightarrow \tilde{f}$, $k \leftrightarrow r$, $N_n \rightarrow \tilde{N_n}$, and $b \rightarrow -b$, we find similar results for the inverse transforms

$$\tilde{f_m}(k) = c \int_0^{\infty} r dr\, J_m(kr)\, f_m(r) \quad , \quad c = 2\pi \tilde{N_n}(a,b)(-bi)^m \;, \tag{25}$$

and

$$\tilde{f_{\ell m}}(k) = c \int_0^{\infty} r^2 dr\, j_{\ell}(kr)\, f_{\ell m}(r) \quad , \quad c = 4\pi \tilde{N_n}(a,b)(-bi)^{\ell} \;. \tag{26}$$

The $n = 3$ cylindrically symmetric $f'_\ell(r)$ and $\tilde{f'_\ell}(k)$ transform identically to $f_{\ell m}(r)$ and $\tilde{f_{\ell m}}(k)$, as given in equations 24 and 26, since they are simply related by an ℓ-dependent rescaling factor.

2 Spherical Bessel Transforms

Our algorithm for evaluating the scaled spherical Bessel transform equations 24 and 26[6] follows earlier work in references [3, 2].

With the change to dimensionless variables

$$\kappa = \log(k/k_0) \quad , \quad \rho = \log(r/r_0) \;, \tag{27}$$

we can write equation 24 as a convolution suitable for FFT evaluation

$$(r/r_0)^{\alpha} \cdot f_{\ell m}(r) = \int_{-\infty}^{+\infty} G(\rho + \kappa) F(\kappa) d\kappa \tag{28}$$

with dimensionless functions

$$G(s) = e^{\alpha s}\, j_{\ell}(k_0 r_0 e^s) \quad , \quad F(s) = c\, e^{(3-\alpha)s}\, k_0^3\, \tilde{f_{\ell m}}(k_0 e^s) \;, \tag{29}$$

[6] Since these are simply related by the substitution $r \leftrightarrow k$, we use the notation of equation 24 in the following, without any loss of generality.

where the r-weighting parameter α is arbitrary at this point. The function F depends on f, but $G(s)$ depends only on the values of $k_0 r_0$ and α (see Fig. 1), and has asymptotes

$$G_+(s) = \frac{1}{k_0 r_0}\, e^{(\alpha-1)s} \quad , \quad G_-(s) = \frac{2^{-(\ell+1)}\sqrt{\pi}}{\Gamma(\ell+3/2)}\,(k_0 r_0)^\ell\, e^{(\alpha+\ell)s}\ , \tag{30}$$

where G_+ is the envelope of oscillations with a rapidly decreasing period $2\pi e^{-s}/(k_0 r_0)$.

In order to simplify the calculations, we use our freedom to chose $k_0 r_0$ and α to symmetrize $G(s)$ via

$$\alpha = \frac{1-\ell}{2} \quad , \quad \left(\frac{k_0 r_0}{2}\right)^{\ell+1} = \frac{\Gamma(\ell+3/2)}{\sqrt{\pi}}\ , \tag{31}$$

which yields

$$G_+(s) = G_-(-s) = \frac{1}{2}\left[\frac{\sqrt{\pi}}{\Gamma(\ell+3/2)}\right]^{1/(\ell+1)} \cdot \exp\left(-(\ell+1)s/2\right)\ . \tag{32}$$

We can write this using

$$s_0 = \frac{2}{\ell+1} \quad , \quad G_0 = \frac{1}{k_0 r_0}\ , \tag{33}$$

as

$$G_+(s) = G_-(-s) = G_0 e^{-s/s_0}\ . \tag{34}$$

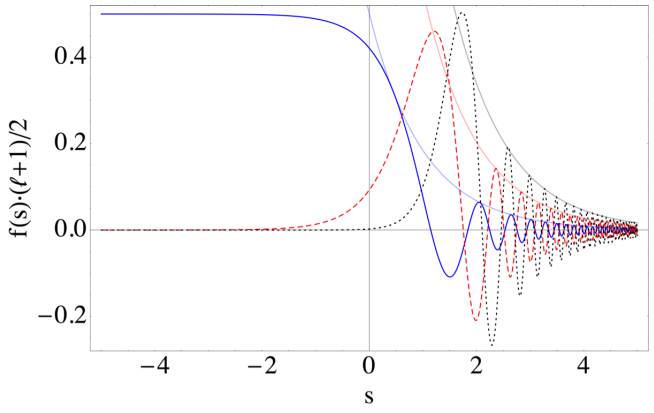

Figure 1: Plots of $f(s)\cdot(\ell+1)/2$ with $\alpha = 0$, $k_0 r_0 = 1$ and $\ell = 0$, 2 (dashed), 4 (dotted). Fainter curves show the large-s asymptotic forms. Left- and right-hand plots are for the spherical Bessel and Hankel transforms, respectively.

3 Hankel Transforms

We use a similar algorithm to calculate the scaled Hankel transforms of equations 23 and 25, using primes to denote cases where the $n = 2$ and $n = 3$ cases differ.

We can transform eqn. 23 to the convolution equation 28 using

$$G'(s) = e^{\alpha s}\, J_\ell(k_0 r_0 e^s) \quad , \quad F'(s) = c e^{(2-\alpha)s}\, k_0^2\, \tilde{f_{\ell m}}(k_0 e^s)\ , \tag{35}$$

where, as above, the $r-$weighting parameter α is arbitrary at this point. Fig. 1 compares this $f(s)$ with the spherical Bessel transform case and shows that they have similar asymptotic behavior:

$$G'_+(s) = \left(\frac{2}{\pi k'_0 r'_0}\right)^{1/2} e^{(\alpha' - \frac{1}{2})s} \quad , \quad G'_-(s) = \frac{2^{-\ell}}{\Gamma(\ell+1)}\,(k'_0 r'_0)^\ell\, e^{(\alpha'+\ell)s}\ . \tag{36}$$

Again, we symmetrize via

$$\alpha' = \frac{1-2\ell}{4} \quad , \quad \left(\frac{k'_0 r'_0}{2}\right)^{\ell+1/2} = \frac{\Gamma(\ell+1)}{\sqrt{\pi}}\ , \tag{37}$$

which yields

$$G'_+(s) = G'_-(-s) = \left[\pi^\ell\, \Gamma(\ell+1)\right]^{-1/(2\ell+1)} \cdot \exp\left(-(2\ell+1)s/4\right)\ . \tag{38}$$

We can rewrite this using

$$s'_0 = \frac{4}{2\ell+1} \quad , \quad G'_0 = \left(\frac{2}{\pi k'_0 r'_0}\right)^{1/2} \quad , \tag{39}$$

as

$$G'_+(s) = G'_-(-s) = G'_0 e^{-s/s'_0}\ . \tag{40}$$

4 Discretization

In order to perform the convolution using FFT, we discretize $s_n = n\Delta s$ with $|n| \le N$, and require that both F and G go to zero outside of the sampled interval (large $s_N = N\Delta s$) and are sampled sufficiently finely (small Δs).

We then pick s_N so that $G(s_N) \simeq \epsilon G(0)$, i.e.,

$$s_N = -s_0\, \log\epsilon + \delta\ , \tag{41}$$

where ϵ is a numerical precision parameter that specifies the fractional level at which we truncate $G(s)$ and we choose $\delta > 0$ so that s_N lands at the next zero of the oscillation (in the limit of small ϵ)

$$e^\delta = \lceil Y \rceil / Y \quad , \quad e^{\delta'} = \frac{\lceil 1/8 + Y'/4 \rceil - 1/8}{Y'}\ , \tag{42}$$

where $\lceil Y \rceil$ is the smallest integer $\geq Y$ with

$$Y \equiv \frac{k_0 r_0}{2\pi} \epsilon^{-s_0} \ . \tag{43}$$

We meet the second condition by requiring n_s samples[7] of the large-s oscillation at s_N. We accomplish this using $\Delta s \leq \Delta s_{\max}$ with

$$\Delta s_{\max} = h\, \epsilon^{s_0} \quad , \quad h \equiv \frac{2\pi}{n_s k_0 r_0} \ . \tag{44}$$

In order to preserve the node at s_N and ensure that N is integral, we pick

$$N_G = \lceil s_N / \Delta s_{\max} \rceil \quad , \quad \Delta s = s_N / N_G \ . \tag{45}$$

Fig. 2 shows examples of $G(s)$ tabulated with these prescriptions. Note that the symmetrized $G(s)$ peaks at small positive s but that the oscillations for $s > 0$ lead to a negative first moment.

We now turn to the discretization of $F(s)$, which depends on an unknown f. Since $s = \kappa$ when evaluating $F(s)$, our choice of Δs above directly determines the sampling of $\tilde{f_{\ell m}}(k)$. To ensure that f is sufficiently sampled, we take

$$\Delta s_{\max} = \min(\frac{\log 10}{N_{10}}, c\epsilon^{s_0}) \tag{46}$$

where N_{10} is the minimum allowed sampling per decade of $\tilde{f_{\ell m}}(k)$.

In practice, we want to know $f_{\ell m}(r)$ over some range $r_{\min} < r < r_{\max}$. Therefore, we set

$$r_0 = \sqrt{r_{\min} r_{\max}} \tag{47}$$

and calculate the corresponding k_0 using the value of $k_0 r_0$ obtained in eqn. (31) or eqn. (37). We want a result that is free of aliasing artifacts over $2N_F$ samples where

$$2N_F = \log(r_{\max}/r_{\min})/\Delta s \ , \tag{48}$$

so we pad the tabulated $G(s_n)$ with $2N_F$ zeros and perform transforms of length $2(N_F + N_G)$. The resulting range of k used in the calculation has limits

$$k_{\min} = k_0 \exp(-(N_F + N_G)\Delta s) \quad , \quad k_{\max} = k_0 \exp(+(N_F + N_G)\Delta s) \ . \tag{49}$$

5 Errors

We have framed our discretization in terms of ϵ but, in practice, a better choice would be $\varepsilon = \Delta s / s_{\max}$ since this more directly correlates with the processing

[7] Nyquist limit sampling corresponds to $n_s = 2$.

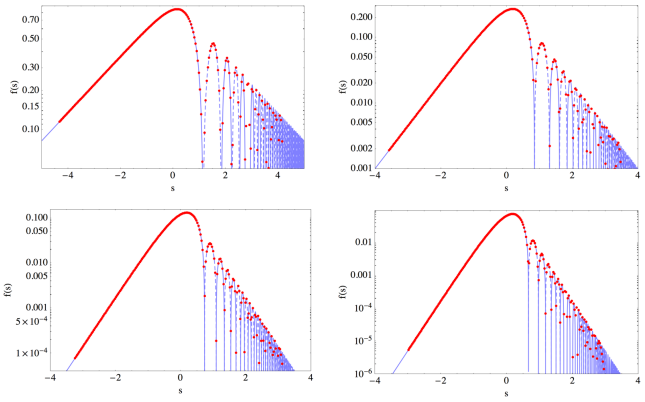

Figure 2: Tabulated values of the symmetrized functions $G(s)$ for $\ell = 0$ (top-left), 2 (top-right), 4 (bottom-left), and 6 (bottom-right). Curves show the functions $G(s)$ on a log scale, using dashing for negative segments of the oscillation, and points show the discretization $|G(s_n)|$ for $|n| \le N$, using $n_s = 2$ and $\varepsilon = 0.01$ ($\epsilon \simeq 1.1 \times 10^{-1}$, 4.7×10^{-3}, 3.2×10^{-4}, 3.0×10^{-5} for $\ell = 0, 2, 4, 6$.)

and memory requirements. Therefore we convert a specified ε into a value of ϵ by inverting

$$\varepsilon = h\, \epsilon^{s_0} / \log \epsilon^{-s_0} \ , \tag{50}$$

which can either be done numerically or else using the approximation

$$\epsilon^{s_0} \simeq -\frac{L_0}{6L_1^3} \left[6L_1^4 + 6L_1^2 L_2(L_1+1) - 3L_1 L_2(L_2-2) + L_2(2L_2^2 - 9L_2 + 6)\right] \ , \tag{51}$$

where

$$L_0 \equiv \varepsilon/h \quad , \quad L_1 \equiv \log(L_0) \quad , \quad L_2 \equiv \log(-L_1) \ , \tag{52}$$

which is valid for $L_0 \lesssim 0.35$. The discretizations in Fig. 2 are calculated with a fixed $\varepsilon = 0.01$, and so have corresponding values of ϵ that increase with ℓ.

In order to provide more direct control of the transform accuracy, we implement a driver routine that starts from some initial ε (nominally 0.01) and then reduces its value by factors until[8]

$$|f_\ell(r_j;\varepsilon) - f_\ell(r_j;2\varepsilon)| < \max\left(e_{\mathrm{abs},\ell} \cdot r_j^p, e_{\mathrm{rel},\ell} \cdot |f_\ell(r_j;\varepsilon)|\right) \tag{53}$$

for all j, where the r_j are equally spaced over the range $r_{\min} \le r \le r_{\max}$ and p allows for an r-weighing of the 'constant' error criterion (but we normally use $p = 0$). We abandon the halving of ε once it reaches some prescribed minimum value (nominally 10^{-6}), to protect against pathological cases.

[8] We assume $n = 3$ with spherical symmetry here for notational convenience.

For the purposes of transforming a set of multipoles that are subsequently recombined using equation 3, 7, or 12, we require that[9]

$$e_{\mathrm{rel},\ell} = \frac{e_{\mathrm{rel}}}{M} \frac{|\sum_{\ell'} f_{\ell'}(r) L_{\ell'}(\mu_r)|}{|f_\ell(r) L_\ell(\mu_r)|} \quad , \quad e_{\mathrm{abs},\ell} = \frac{e_{\mathrm{abs}}}{M} \, , \tag{54}$$

for all (r, μ_r) on a grid covering the region of interest, where M is the number of multipoles included in the expansion.

References

[1] Scott Dodelson. *Inhomogeneities*. Elsevier, 2003.

[2] A. J. S. Hamilton. Uncorrelated modes of the non-linear power spectrum. *Monthly Notices of the Royal Astronomical Society*, 312(2):257–284, Feb 2000.

[3] J.D. Talman. NumSBT: A subroutine for calculating spherical Bessel transforms numerically. *Computer Physics Communications*, 180(2):332–338, Feb 2009.

[4] David H. Weinberg, Michael J. Mortonson, Daniel J. Eisenstein, Christopher Hirata, Adam G. Riess, and Eduardo Rozo. Observational probes of cosmic acceleration. *Physics Reports*, 530(2):87–255, Sep 2013.

[9] We assume $n = 3$ with spherical symmetry here for notational convenience.